Analytical Parameter Extraction of the HBT Equivalent Circuit with T-Like Topology from Measured S-Parameters

Ulrich Schaper, *Member, IEEE,* and Birgit Holzapfl

***Abstract*—A pure analytical method for extraction of the small-signal equivalent circuit parameters from measured data is presented and successfully applied to heterojunction bipolar transistors (HBT's). The T-like equivalent circuit is cut into three shells accounting for the connection, and the extrinsic and intrinsic parts of the transistor. The equivalent circuit elements are evaluated in a straightforward manner from impedance and admittance representation of the measured S-parameters. The measured data are stripped during the extraction process yielding, step by step, a full set of circuit elements without using fit methods. No additional knowledge of the transistor is needed to start the extraction process with its self-consistent iteration loop for the connection shell. The extrinsic and intrinsic equivalent circuit elements are evaluated using their bias and frequency dependencies. This method yields a deviation of less then 4% between measured and modeled S-parameters.**

I. Introduction

HETEROJUNCTION bipolar transistors (HBT's) based on III-V materials are used for digital, analog, and power applications due to their excellent switching speed combined with high current driving capability [1], [2]. In the case of monolithic microwave integrated circuit (MMIC) applications, a large-signal model has to be used in order to describe the active HBT properties over the total operating bias range from dc to more than 20 GHz. The HBT is characterized at many bias settings by S-parameter measurements over the frequency range of interest. All these measurement data can be reduced at any bias to a set of 15 frequency-independent parameters using a small-signal equivalent circuit with T-like topology. This topology has been used successfully by many authors [3]–[5]. We have shown that this equivalent circuit can describe the scaling behavior of the HBT with physically meaningful elements [6]. In all these cases, the parameter values were found by fitting methods, i.e., minimization of an error function using optimizers. The disadvantage of this method is that the optimizer is operating in a mathematical parameter space with 15 dimensions which usually has many minima. In order to obtain a minimum which makes sense from a physical or circuit application point of view, suitable starting values for the optimization [7] are essential.

Manuscript received February 8, 1993; revised July 11, 1994. This work was supported by the BMFT, Bonn, Germany, under Contract TK 034518.

The authors are with Corporate Research and Development, Department ZFE ST KM 5, Siemens AG, D-81730 Munich, Germany.

IEEE Log Number 9407441.

In this paper we propose an analytical determination of the parameter values of the intrinsic and extrinsic transistor directly from the S-parameters measured in the range of 1–26 GHz. This method avoids the multiple minima problem by a definite extraction of the parameter values. An open structure may be used for transistors with a small emitter area as an additional test structure for the de-embedding of the S-parameters from the parasitic environment due to on-wafer measurements and interconnect metallization [8]. For the parameter extraction, the bipolar transistor is measured in the active mode at several bias points to distinguish between bias dependent and independent elements. In case of FET modeling, this corresponds to the cold-FET measurement [9], [10]. A cutoff mode modeling of HBT's has been discussed in [11], but only with emphasis on de-embedding techniques. For circuits without the extrinsic collector capacitance, a method to constrain the elements during an optimization procedure [12] is based on analysis of the delay times composing the transit frequency of the device. An analytical extraction technique is proposed in [13] based on a circuit without the extrinsic collector capacitance which displays a coupling between input and output of the two-port description. This capacitance is included in our method and directly calculated from the admittance description of the transistor. The emitter series resistance is essential for a precise modeling of the bipolar transistor. An analytical method to extract this bias independent resistance has been shown by Maas [14]. For the hybrid-pi representation of the bipolar transistor, a direct extraction method is given in [15], but further measurements on additional test structures are necessary for this parameter extraction of the extrinsic transistor.

II. Theoretical Analysis

The small-signal equivalent circuit is shown in Fig. 1. The two-port behavior can be described either by impedance ($\underline{\underline{Z}}$) or admittance ($\underline{\underline{Y}}$) matrices which can be converted to the S-parameter matrix. The equivalent circuit is built up to three parts like shells. The inner part denoted by $\underline{\underline{Z}}_i$ (dotted box in Fig. 1) represents the intrinsic transistor. The emitter impedance Z_F and collector impedance Z_Q represent the p-n-junctions. The current source is described by the dc-current gain α_0 and a rolloff frequency f_α. The internal series

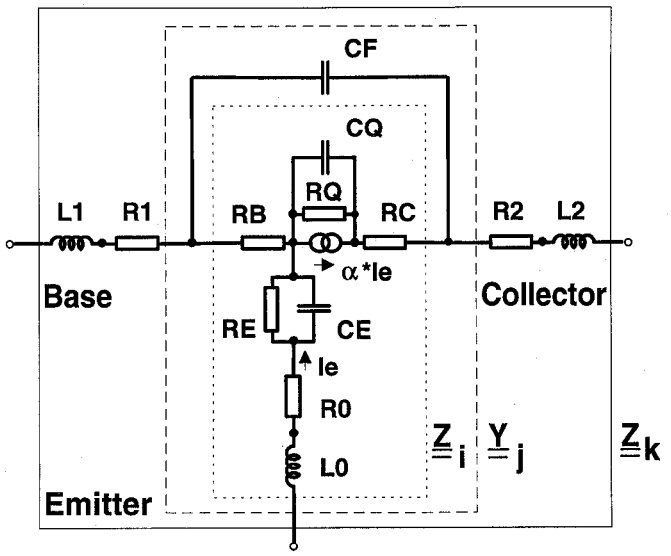

Fig. 1. Small-signal equivalent circuit with T-like topology. The three shells composing the circuit are denoted by the impedance or admittance matrices $\underline{\underline{Z}}_i$ (dotted), $\underline{\underline{Y}}_j$ (dashed), and $\underline{\underline{Z}}_k$, respectively.

resistances of the base and collector layers are Z_B and Z_C

$$\underline{\underline{Z}}_i = \begin{pmatrix} Z_E + Z_B & Z_E \\ Z_E - \alpha Z_Q & Z_E + Z_Q + Z_C - \alpha Z_Q \end{pmatrix} \tag{1}$$

$$Z_E = R_0 + j\omega L_0 + \frac{1}{\frac{1}{R_E} + j\omega C_E} \tag{2}$$

$$Z_Q = \frac{1}{\frac{1}{R_Q} + j\omega C_Q} \tag{3}$$

$$Z_B = R_B \tag{4}$$

$$Z_C = R_C \tag{5}$$

$$\alpha = \frac{\alpha_0}{1 + j\frac{\omega}{2\pi f_\alpha}}. \tag{6}$$

For devices with many fingers, an emitter inductance L_0 has been added in series to R_0. The base collector capacitance of the extrinsic transistor C_F is parallel to the internal transistor, both build up the second shell of the equivalent circuit, which is described by $\underline{\underline{Y}}_j$ (dashed box in Fig. 1)

$$\underline{\underline{Y}}_i = \frac{1}{\det(\underline{\underline{Z}}_i)} \begin{pmatrix} Z_E + Z_Q + Z_C - \alpha Z_Q & -Z_E \\ -Z_E + \alpha Z_Q & Z_E + Z_B \end{pmatrix} + \frac{1}{Z_F} \begin{pmatrix} 1 & -1 \\ -1 & 1 \end{pmatrix} \tag{7}$$

$$Z_F = \frac{1}{j\omega C_F}. \tag{8}$$

The outer shell of the equivalent circuit is then built up by adding the external base (Z_1) and collector (Z_2) impedances. The impedance matrix $\underline{\underline{Z}}_k$ of the whole equivalent circuit is given by (9), shown at the bottom of the page

$$Z_1 = R_1 + j\omega L_1 \tag{10}$$

$$Z_2 = R_2 + j\omega L_2. \tag{11}$$

For simplicity, we have used only one index for each element, the physical interpretation can be done by referring to the circuit and device topology [6].

III. Parameter Extraction

The construction of two-port matrices from the inner shell to the outer one is an easy way to go. The measured data of the transistor are described by the outer shell given by the complicated matrix $\underline{\underline{Z}}_k$. Now one has to go step by step from the measured data to the inner shell and to the single circuit elements.

A. Extrinsic Transistor

The first step is to extract Z_1 and Z_2

$$Z_{k11} - Z_{k12} = Z_1 + \frac{Z_F Z_B}{Z_F + Z_Q + Z_C + Z_B} \tag{12}$$

$$Z_{k22} - Z_{k21} = Z_2 + \frac{Z_F(Z_Q + Z_C)}{Z_F + Z_Q + Z_C + Z_B}. \tag{13}$$

The differences of the $\underline{\underline{Z}}_k$ matrix elements given Z_1 and Z_2 can be approximated by

$$Z_{k11} - Z_{k12} \approx R_1 + j\omega L_1 + R_B\frac{C_Q}{C_F} - j\frac{1}{\omega C_F}\frac{R_B}{R_Q} \tag{14}$$

$$Z_{k22} - Z_{k21} \approx R_2 + j\omega L_2 - R_B\frac{C_Q}{C_F} + \frac{1}{R_Q(\omega C_F)^2} - \frac{j}{\omega C_F}\left(1 - \frac{C_Q}{C_F}\right). \tag{15}$$

The approximations in (14) and (15) are based on the assumptions (16)–(19):

$$R_Q \gg \frac{1}{\omega C_Q} \tag{16}$$

$$R_B + R_C \ll \frac{1}{\omega C_F} \tag{17}$$

$$\frac{C_Q}{C_F} \ll 1 \tag{18}$$

$$R_C \ll \frac{1}{\omega C_Q}. \tag{19}$$

$$\underline{\underline{Z}}_k = \begin{pmatrix} Z_1 + Z_E + Z_B - \frac{Z_B(Z_B - \alpha Z_Q)}{Z_F + Z_Q + Z_C + Z_B} & Z_E + \frac{Z_B(Z_Q + Z_C - \alpha Z_Q)}{Z_F + Z_Q + Z_C + Z_B} \\ Z_E + \frac{Z_B(Z_Q + Z_C - \alpha Z_Q)}{Z_F + Z_Q + Z_C + Z_B} - \frac{Z_F \alpha Z_Q}{Z_F + Z_Q + Z_C + Z_B} & Z_2 + Z_E + \frac{(Z_F + Z_B)(Z_Q + Z_C - \alpha Z_Q)}{Z_F + Z_Q + Z_C + Z_B} \end{pmatrix} \tag{9}$$

TABLE I
THE MODEL PARAMETERS WITH THEIR MEAN VALUES AND STANDARD DEVIATIONS ARE GIVEN AFTER THE BIAS ANALYSIS IS PERFORMED FOR THREE DIFFERENT BIAS CONDITIONS

bias				
V_{CE}	V	1.0	1.0	1.0
I_C	mA	6.7	13.2	19.0
parameter	unit			
R_1	Ω	3.6 ± 0.4	3.6 ± 0.4	3.6 ± 0.4
L_1	pH	62. ± 3.	63. ± 4.	62. ± 5.
R_2	Ω	4.7 ± 0.5	4.7 ± 0.5	4.7 ± 0.5
L_2	pH	65. ± 7.	54. ± 6.	60. ± 4.
C_F	fF	51. ± 1.	54. ± 1.	61. ± 1.
R_0	Ω	2.0 ± 0.3	2.0 ± 0.3	2.0 ± 0.3
L_0	pH	< 1.	< 1.	< 1.
R_C	Ω	0.6 ± 0.4	0.6 ± 0.4	0.6 ± 0.4
R_B	Ω	14.4 ± 0.7	11.1 ± 0.6	8.4 ± 0.5
R_E	Ω	5.4 ± 0.6	2.4 ± 0.3	1.4 ± 0.2
C_E	pF	2.1 ± 0.6	3.8 ± 1.	2.9 ± 0.8
R_Q	kΩ	22. ± 1.	11.2 ± 0.7	7.5 ± 0.3
C_Q	fF	2.8 ± 0.1	2.7 ± 0.1	3.1 ± 0.1
α_0		0.866±0.005	0.870 ± 0.003	0.863 ± 0.003
f_α	GHz	35. ± 2.	43. ± 1.	45. ± 1.
S-parameter				
mean error	%	4.9	3.9	5.4

The calculation of Z_1 and Z_2 from the differences of the $\underline{\underline{Z}}_k$ matrix elements includes corrections by R_B, R_Q, C_Q, and C_F. Two pieces of information on these 4 elements can be extracted already from the outer shell. The ratio C_Q/C_F is given by

$$\mathrm{Im}\{(Z_{k22}-Z_{k21})\} \approx -\frac{1}{\omega C_F}\left(1-\frac{C_Q}{C_F}\right) \qquad \text{Freq} < 16\,\text{GHz} \quad (20)$$

and R_Q can be extracted in the low-frequency range

$$\mathrm{Re}\{(Z_{k22}-Z_{k21})\} \approx \frac{1}{R_Q(\omega C_F)^2} \qquad \text{Freq} < 10\,\text{GHz}. \quad (21)$$

The remaining two pieces of information have to be extracted from the intermediate shell $\underline{\underline{Y}}_j$

$$Y_{j12} \approx -j\omega C_F. \quad (22)$$

Now, R_Q and C_Q are known by (21), (22), and (20), so R_B can be determined either from the real or imaginary part of (23).

$$\frac{Y_{j11}+Y_{j21}}{Y_{j22}+Y_{j12}} \approx \frac{1}{R_B R_Q}\frac{1}{\left(\frac{1}{R_Q^2}+(\omega C_Q)^2\right)} - j\frac{1}{R_B}\frac{\omega C_Q}{\left(\frac{1}{R_Q^2}+(\omega C_Q)^2\right)}. \quad (23)$$

For the approximations in (22) and (23), two assumptions in addition to (16)–(19) are used: $R_C \ll R_Q$, and $\omega C_E < 1/R_E$. All assumptions made are fulfilled for the devices considered. This can be checked by the parameters of the example given in Table I.

For a fixed bias point, an iterative procedure is established beginning with the determination of Z_1 and Z_2 from (14) and (15) with R_B and $1/C_F$ assumed to be zero. Then the parameters C_F, C_Q, R_Q, and R_B are calculated from (20)–(23). These values are used for the correction of Z_1 and Z_2. This iteration loop converges within a few iteration steps. The sensitive test parameter for the convergence of the iteration loop is the capacity C_F. If the values for the external base and collector impedances are extracted correctly, then $\mathrm{Im}\{Y_{j12}\}$ from the intermediate shell shows a capacitive behavior over a wide frequency range describing C_F.

B. Intrinsic Transistor

Once the elements of the outer and intermediate shells are determined, the circuit elements of the inner shell are calculated directly from $\underline{\underline{Z}}_i$. The value of R_B extracted from $\underline{\underline{Z}}_i$

$$R_B = \mathrm{Re}\{Z_{i11}-Z_{i12}\} \quad (24)$$

is very close to the value extracted from $\underline{\underline{Z}}_k$, which confirms the consistency of the extraction procedure for the extrinsic transistor. The emitter resistances R_E and R_0 are in series; they are given by

$$R_E + R_0 = \mathrm{Re}\{Z_{i12}\}. \quad (25)$$

The resistance R_0 represents contact and sheet resistance which is bias independent. The base-emitter resistance R_E varies with $1/I_E$. Parameter extractions at different bias settings are done as proposed by Maas [14]. To distinguish between resistances in series, R_0+R_E is plotted versus $1/I_E$. Once R_E is known, C_E follows from

$$\omega C_E R_E^2 = -\mathrm{Im}\{Z_{i12}\}. \quad (26)$$

R_Q and C_Q are determined from

$$R_Q = \frac{1}{\mathrm{Re}\left\{\frac{1}{Z_{i22}-Z_{i21}}\right\}} \quad (27)$$

$$\omega C_Q = \mathrm{Im}\left\{\frac{1}{Z_{i22}-Z_{i21}}\right\} \quad (28)$$

which again are used to control the values extracted from the extrinsic transistor. R_C is determined from a measurement in cutoff mode to distinguish this parameter from extrinsic resistance R_2. The error of R_C is difficult to reduce since R_C and R_Q are connected in series. The remaining parameters α_0 and f_α of the current source are calculated from Z_{i21} using Z_{i12} and Z_{i22}

$$\alpha_0 = \mathrm{Re}\left\{\frac{Z_{i12}-Z_{i21}}{Z_{i22}-Z_{i21}}\right\} \quad (29)$$

$$f_\alpha = \frac{-\alpha_0 f}{\mathrm{Im}\left\{\frac{Z_{i12}-Z_{i21}}{Z_{i22}-Z_{i21}}\right\}}. \quad (30)$$

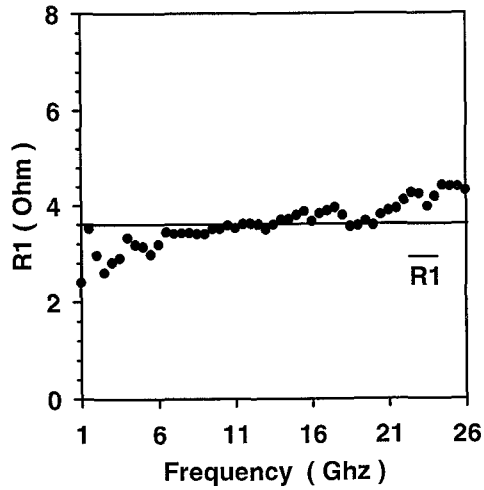

Fig. 2. External series resistance R_1 of the base contact versus frequency. For each measured frequency f, there is a parameter value $R_1(f)$ extracted from impedance matrix $\underline{\underline{Z}}_k$. The frequency independent mean value is $\overline{R_1}$.

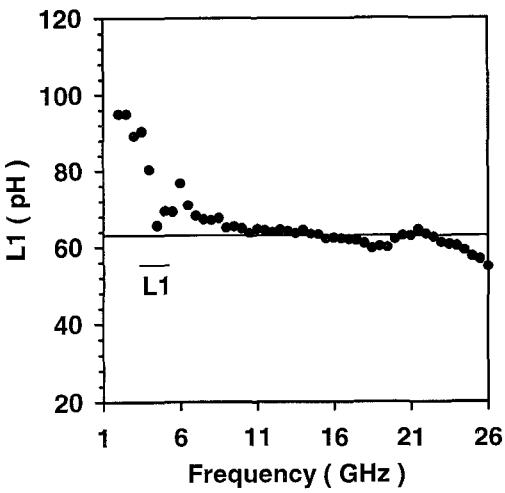

Fig. 3. Inductance L_1 of the base contact versus frequency. The inductance $L_1(f)$ is directly calculated for each measured frequency f from the impedance matrix $\underline{\underline{Z}}_k$; the mean value $\overline{L_1}$ is displayed as a straight line. The reactance ωL_1 is of the same order of magnitude as the series resistance R_1.

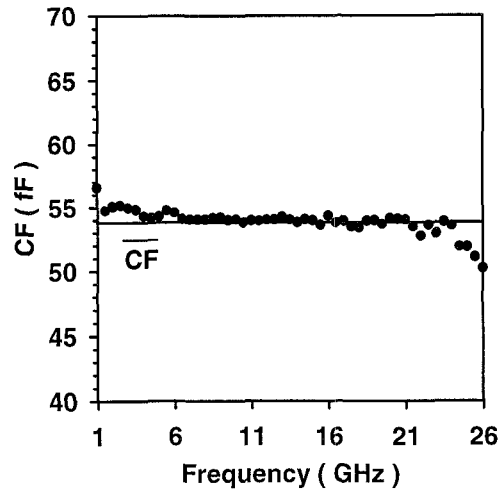

Fig. 4. Capacitance C_F of the extrinsic transistor versus frequency. The coupling capacitance $C_F(f)$ between input and output of the two-port is extracted for each frequency f from the admittance matrix $\underline{\underline{Y}}_j$ describing the intermediate shell. The mean value $\overline{C_F}$ is determined over the whole frequency range.

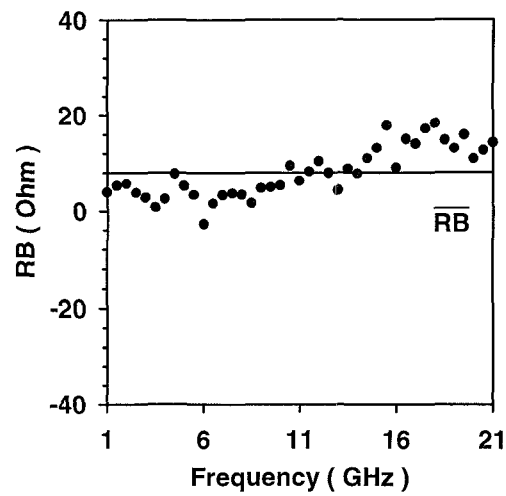

Fig. 5. Internal base series resistance R_B versus frequency before the bias analysis is performed. $R_B(f)$ is determined from the impedance matrix $\underline{\underline{Z}}_i$ of the inner shell at each frequency; the frequency mean value is $\overline{R_B}$.

IV. Measurements and Results

Several different types of HBT's have been investigated to verify the proposed extraction technique. We examined one-emitter-finger HBT's based on the material system GaInP/GaAs [6] (emitter area $A_E = 2.5*21\ \mu m^2$, $2.5*100\ \mu m^2$) as well as multiemitter-finger HBT's based on the material system AlGaAs/GaAs ($A_E = 10*1.5*22.5\ \mu m^2$, $16*2*20\,\mu m^2$). For HBT's with only one emitter-finger, the emitter inductance L_0 is less than 1 pH and can be omitted. For all these types of HBT's, the measurements are described very well qualitatively and quantitatively by the extracted parameters. The measurements were done on-wafer with a microwave probing system. The frequency range was 1–26 GHz for all measurements. The $S-$parameters were measured at several bias settings including the cutoff mode with $V_{CE} = 0$ V, $V_{BE} = 0$ V.

Results of the extraction procedure are discussed for a one-emitter-finger HBT with 52.5 μm^2 emitter area. Beginning with the outer shell of the equivalent circuit, the frequency dependences of R_1 and L_1 are calculated. The parameter values $R_1(f)$ and $L_1(f)$ extracted at each measured frequency f are plotted versus the frequency in Figs. 2 and 3. Together with these values, the frequency independent mean values $\overline{R_1}$ and $\overline{L_1}$ are displayed as straight lines. After two steps of the iteration as described above, the extrinsic collector capacitance C_F is then already frequency independent up to 24 GHz (Fig. 4), which is sufficient for the remaining steps in the parameter extraction. Once the model parameter Z_1, Z_2, and C_F are known (see Table I), the inner shell of the circuit is reached. Examples of the model parameters of the inner part of the circuit are shown in Figs. 5 and 6 for R_B and C_Q versus frequency f; the rolloff frequency f_α of the current source is shown in Fig. 7. The model parameter values are listed in Table I together with their standard deviation over the frequency range at three different bias points.

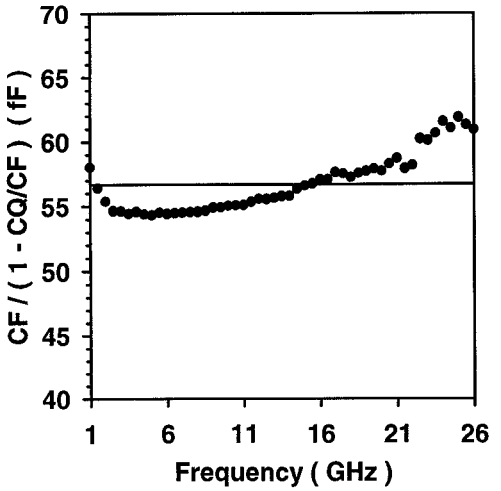

Fig. 6. Capacitance $C_F/(1-C_Q/C_F)$ versus frequency. $\overline{C_Q}$ is calculated from the mean value and the known value of C_F.

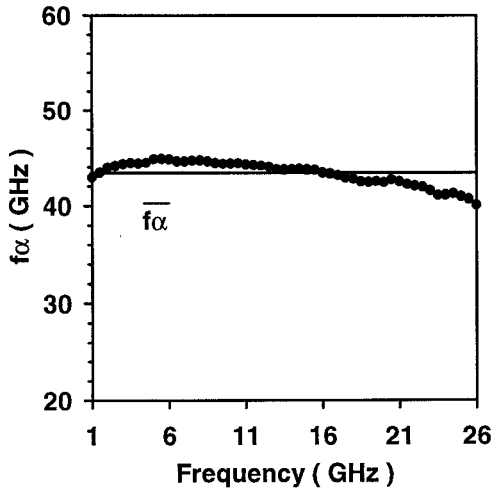

Fig. 7. Rolloff frequency f_α of the current source versus frequency. $f_\alpha(f)$ is extracted as the last parameter from the inner part of the equivalent circuit. The frequency independency of the mean value f_α displays a consistent overall description of the transistor by the model.

The next step is then to go through the extraction method at different bias points. The sum of the resistances $R_0 + R_E$ is plotted versus $1/I_E$ (Fig. 8) to extract the bias independent parameter $R_0 = 2.2\ \Omega$. This procedure reduces the variance of these resistances significantly. A corresponding analysis is done for the contact and sheet resistances R_1 and R_2. R_1 is connected with the bias dependent parameter R_B and C_F (Fig. 1) and described by (12) and (14). Plotting the real part of the difference $Z_{k11} - Z_{k12}$ versus the base current (Fig. 9) gives the bias independent value of R_1. In this way, the variance of the internal resistance R_B is reduced significantly. R_2 and R_C are considered in the same way. The frequency independent mean values of the extracted model parameters have to describe the measured S-parameters of the transistor. A comparison between measured and modeled S-parameters shows a very good agreement (Fig. 10) for all four complex S-parameters with an error of only 4%; the main contribution to this error comes from s_{21}. This parameter set has been achieved without any fit. The highest deviation occurs at the high-frequency end where the simple circuit we have used may be modified.

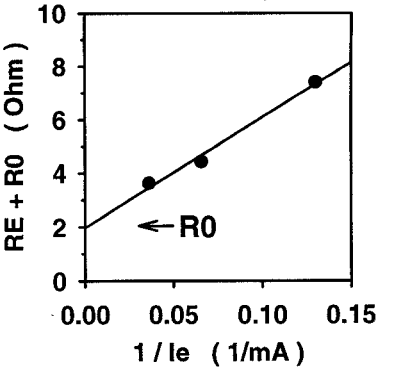

Fig. 8. The total emitter resistances $R_0 + R_E$ versus inverse emitter current. The bias independent value of R_0 is 2 Ω.

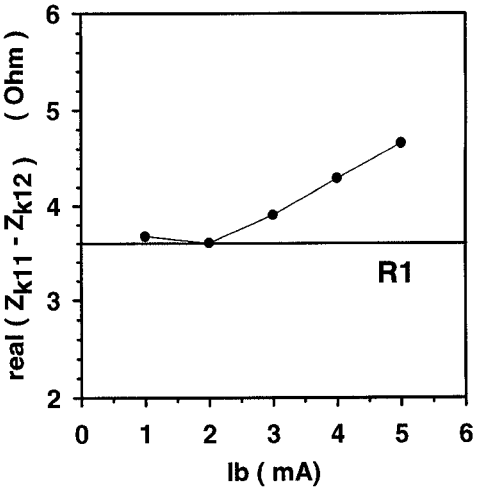

Fig. 9. Difference of the matrix elements $Z_{k11} - Z_{k12}$ (12) versus base current. The bias independent real input resistance R_1 is 3.6 Ω.

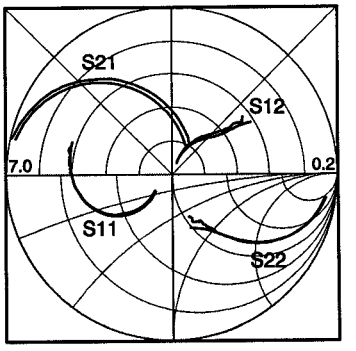

Fig. 10. Comparison of the measured and modeled S-parameters for $I_c = 13.2$ mA. The lower part of the figure shows a Smith diagram with S_{11} and S_{22}. The measured values can be identified by small measurement uncertainties in the high-frequency range. The upper part shows a polar plot for S_{21} with a radius of 7; S_{12} in the upper right part uses a radius of 0.2.

V. Conclusion

An efficient method to determine the small-signal equivalent circuit of bipolar transistors especially for microwave HBT's is presented. The equivalent circuit elements can be determined

unambiguously. This is not possible with fitting programs using arbitrary starting conditions. The validity of the description of the transistor by the equivalent circuit is demonstrated by plotting the element values versus frequency. Comparing measured and modeled S-parameters, the average error is less than 4%. This method has been applied successfully to several HBT's including multiemitter devices for power applications.

ACKNOWLEDGMENT

The authors would thank P. Zwicknagl and M. Kärner for encouraging discussions, H. Siweris for S-parameter measurements, and the referee for constructive suggestions.

REFERENCES

[1] M. E. Kim, B. Bayraktaroglu, and A. Gupta, "HBT devices and applications," in *HEMTs & HBTs: Devices, Fabrication, and Circuits,* F. Ali and A. Gupta, Eds. Norwood, MA: Artech House, 1991, pp. 253–369.

[2] M. B. Das, "HBT device physics and models," in *HEMTs & HBTs: Devices, Fabrication, and Circuits,* F. Ali and A. Gupta, Eds. Norwood, MA: Artech House, 1991, pp. 191–251.

[3] R. Ramachandran, M. Nijjar, A. Podell, E. Stoneham, S. Mitchell, N. L. Wang, W. J. Ho, M. F. Chang, G. J. Sullivan, J. A. Higgins, and P. M. Asbeck, "A high-efficiency HBT MMIC power amplifier," in *GaAs IC Symp. 1990 Dig.,* 1990, pp. 357–360.

[4] M. Rodwell, J. F. Jensen, W. E. Stanchina, R. A. Metzger, D. B. Rensch, M. W. Pierce, T. V. Kargodorian, and Y. K. Allen, "33 GHz monolitihic cascode AlInAs/GaInAs heterojunction bipolar transistor feedback amplifier," in *Proc. IEEE Bipolar Circuits Technol. Meet.,* 1990, pp. 252–255.

[5] K. W. Kobayashi, D. K. Umemoto, R. Esfandiari, A. K. Oki, L. M. Pawlowicz, M. E. Hafizi, L. Tran, J. B. Camou, K. S. Stolt, D. C. Streit, and M. E. Kim, "GaAs HBT MMIC broadband amplifiers from DC to 20 GHz," in *Proc. IEEE Microwave Millimeter-Wave Monolithic Circuits Symp.,* 1990, pp. 19–22.

[6] U. Schaper, K. H. Bachem, M. Kärner, and P. Zwicknagl, "Scaling of small-signal equivalent circuit elements for GaInP/GaAs hole-barrier bipolar transistors (HBBT)," *IEEE Trans. Electron Dev.,* vol. 40, pp. 222–224, Jan. 1993.

[7] G. L. Bilbro, M. B. Steer, R. J. Trew, C.-R. Chang, and S. G. Skaggs, "Extraction of the parameters of microwave transistors using tree annealing," *IEEE Trans. Microwave Theory Tech.,* vol. 38, pp. 1711–1718, Nov. 1990.

[8] H. Cho and D. Burk, "A three-step method for the de-embedding of high-frequency S-parameter measurements," *IEEE Trans. Electron Dev.,* vol. 38, pp. 1371–1375, June 1991.

[9] G. Dambrine, A. Cappy, F. Heliodore, and E. Playez, "A new method for determining the FET small-signal equivalent circuit," *IEEE Trans. Microwave Theory Tech.,* vol. MTT-36, pp. 1151–1159, July 1988.

[10] M. Berroth and R. Bosch, "Broad-band determination of the FET small-signal equivalent circuit," *IEEE Trans. Microwave Theory Tech.,* vol. 38, pp. 891–895, July 1990.

[11] S. Lee and A. Gopinath, "Parameter extraction technique for HBT equivalent circuit using cutoff mode measurement," *IEEE Trans. Microwave Theory Tech.,* vol. 40, pp. 574–577, Mar. 1992.

[12] R. J. Trew, U. K. Mishra, W. L. Pribble, and J. F. Jensen, "A parameter extraction technique for heterojunction bipolar transistors," in *IEEE MTT-S Dig.,* 1989, pp. 897–900.

[13] D. R. Pehlke and D. Pavlidis, "Direct calculation of the HBT equivalent circuit from measured S-parameters," in *IEEE MTT-S Dig.,* 1992, pp. 735–738.

[14] S. A. Maas and D. Tait, "Parameter extraction method for heterojunction bipolar transistors," *IEEE Microwave and Guided Wave Lett.,* vol. 2, Dec. 1992.

[15] D. Costa, W. U. Liu, and J. S. Harris, "Direct extraction of the AlGaAs/GaAs heterojunction bipolar transistor small-signal equivalent circuit," *IEEE Trans. Electron Dev.,* vol. 38, pp. 2018–2024, Sept. 1991.

Ulrich Schaper (M'91) received the diploma in physics from the University of Munich, Germany, in 1976 and the Ph.D. degree from the Technical University of Munich in 1981.

He worked at the Max-Planck Institute for Plasma Physics in Garching near Munich on nuclear fusion research. He spent the following years as an assistant researcher at the Institute for Theoretical Physics of the University of Düsseldorf, concerned with the stability of plasma equilibria for nuclear fusion applications. In 1984 he joined the component division of the Siemens AG in Munich, working on SPICE models for MOSFET's. Since 1986 he has been with the Siemens Research Laboratories, where he is responsible for the modeling of heterobipolar transistors.

Birgit Holzapfl graduated from the Engineering School of Siemens AG, Munich, Germany.

In 1983 she joined the Siemens Research Laboratory. From 1983 to 1985 she worked on the development of surface wave filters. Since 1986 she has been engaged in the research of GaAs hetereostructure devices. Currently, she is involved in MMIC design and CAD.